Proceedings of the Fourth
Rochester Conference on
Coherence and Quantum Optics

LBL-6918

SECOND-ORDER SUM- AND DIFFERENCE-FREQUENCY GENERATION VIA QUADRUPOLE TRANSITIONS IN ATOMIC VAPORS

Donald Bethune, Robert W. Smith, and Y. R. Shen

SEPTEMBER 1977

Prepared for the U. S. Energy Research and
Development Administration under Contract W-7405-ENG-48

Y. R. Shen
Signature

SECOND-ORDER SUM- AND DIFFERENCE-FREQUENCY GENERATION VIA QUADRUPOLE TRANSITIONS IN ATOMIC VAPORS

Donald Bethune, Robert W. Smith, and Y. R. Shen

University of California, Berkeley, California

Atomic vapors have played an important role in recent work on optical mixing. They have been used to generate tunable IR radiation, tunable vacuum UV, and coherent radiation with wavelengths as short as 380 Å. Until recently, the schemes used all involved susceptibilities derived by keeping only the dipole interaction of light with the medium. Recently we reported second order sum-frequency generation in Na vapor.[1] The dipole susceptibility for second order mixing vanishes for a vapor, and a more general type of susceptibility must be considered to describe this process.[2] For example, our Na sum-frequency generation can be described as phase matched emission from oscillating atomic quadrupole moments driven at frequency $\omega_3 = \omega_1 + \omega_2$ by two *applied fields*, as shown schematically in Fig. 1. The quadrupole moment density is given by:

$$\underline{Q} = \underline{\underline{\chi}}^{(Q)} : \underline{E}_1\underline{E}_2$$
$$= \chi^{(Q)} \left[\underline{E}_1\underline{E}_2 + \underline{E}_2\underline{E}_1 - \frac{2}{3}\underline{\underline{I}}\,(\underline{E}_1\cdot\underline{E}_2)\right] . \qquad (1)$$

The second form shows that the spherical symmetry of the atoms allows us to define a *scalar* susceptibility, and to derive the quadrupole geometry directly from the incident field vectors. The quadrupole radiation with ~~k-vector~~ $\underline{k}_3 = n_3\omega_3/c\ \hat{e}_3$ is equivalent to that radiated by dipole of strength

$$\underline{P}_{eff} = -i\underline{k}_3 \cdot \underline{Q}$$
$$= -i\chi^{(Q)}[(\underline{k}_3 \cdot \underline{E}_1)\underline{E}_2 + (\underline{k}_3 \cdot \underline{E}_2)\underline{E}_1 - \tfrac{2}{3}(\underline{E}_1 \cdot \underline{E}_2)\underline{k}_3] . \qquad (2)$$

The dot products in Eq.(2) show immediately that a non-collinear geometry must be used, and can also be used to show that the sum-

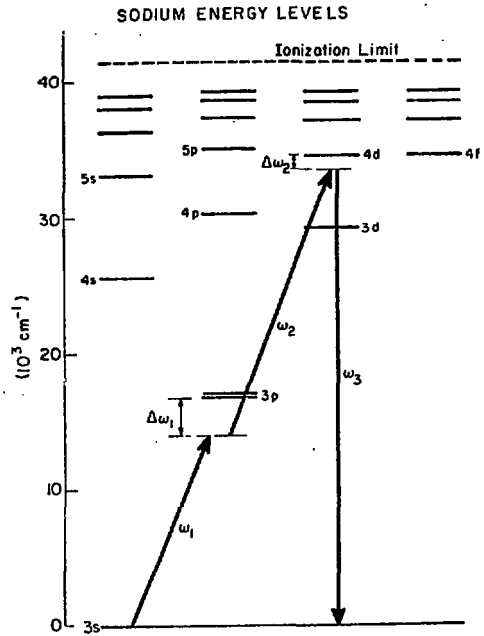

Figure 1: Partial level diagram of the sodium atom. Quadrupole sum-frequency generation with $\omega_3 = \omega_2 + \omega_1$ is shown schematically.

frequency is maximum for orthogonally polarized beams. The output power can be explicitly calculated. The quadrupole susceptibility is given by

$$\chi^{(Q)} = \frac{Ne^3}{\hbar^2} \sum_{rst} \left[\frac{\langle r|yz/2|s\rangle\langle s|y|t\rangle\langle t|z|r\rangle}{(\omega_{sr}-\omega_1-\omega_2-i\gamma)(\omega_{tr}-\omega_1)} + (1 \leftrightarrow 2) \right] , \qquad (3)$$

which can be evaluated using tabulated matrix elements. We find the

output power can be expressed as

$$\mathcal{P}(\omega_3) = \frac{4\pi^5\omega_3^4}{c^5} |\chi^{(Q)}|^2 \mathcal{P}(\omega_1)\mathcal{P}(\omega_2)\ e^{-\Delta k_z^2/2\sigma_k^2} \quad , \qquad (4)$$

where $\Delta k_z = |\underline{k}_3 - \underline{k}_1 - \underline{k}_2|$ is the wave vector mismatch. For example, for Na with $N = 10^{16}$ cm^{-3}, $\gamma_{Laser} = .25$ cm^{-1} and $\omega_3 p_{\frac{1}{2}} - \omega_1 = 10$ cm^{-1}, $\chi^{(Q)} = 3 \times 10^{-14}$ esu, which gives an effective dipole susceptibility $|k_3\chi^{(Q)}| \approx 10^{-9}$ esu, as large as $\chi^{(2)}$ for quartz, ~~Equation (4)~~ Eq. (4) then gives $\mathcal{P}(\omega_3) = \mathcal{P}(\omega_1)\mathcal{P}(\omega_2)/(11.7 \times 10^6)$ watts.

The experimental arrangement used to observe quadrupole sum-frequency generation is shown in Fig. 2. Generally the characteristics of the observed output agree with those predicted by Eq. (4). In particular, the output shows the sharp two-photon resonance expected from the expression for $\chi^{(Q)}$ when $\omega_1 + \omega_2 = \omega_{4d}$ (Fig. 3), and also shows the expected variation with $\underline{k}$ vector mismatch, which is adjusted by changing the beam intersection angle (Fig. 4).

At high densities and high input powers, however, deviations from the simple theory occur, and the output is less than one would expect from Eq. (4). First, with increasing densities, the linear absorption associated with the D-line resonances causes the output

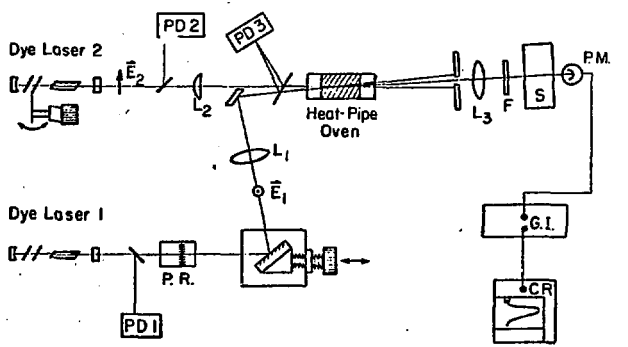

Figure 2: Experimental set-up. PD1, PD2, PD3- monitor photodetectors; L_1, L_2 - 40 cm and 50 cm lenses; L_3 - 10 cm quartz lens; PR - polarization rotator; F- Corning 7-54 filter and pyrex attenuators; S - 25 cm spectrometer; PM - RCA 4837; G. I.- gated integrator; CR - chart recorder.

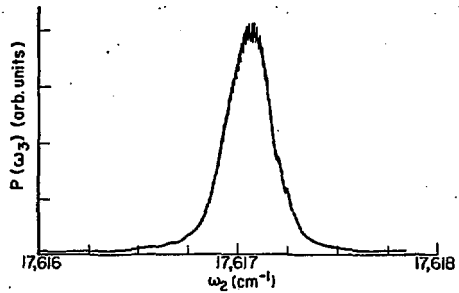

Figure 3: Sum-frequency output $\mathcal{P}(\omega_3)$ as a function of ω_2 showing the sharp resonance at $\omega_1 + \omega_2 = \omega_{4d} = 34548.8$ cm^{-1}. $\mathcal{P}_1 = 2$W; $\mathcal{P}_2 = 25$W; $\theta = 47.9$ mrad; $N = 1.6 \times 10^{16}$ cm^{-3}.

to fall sharply as shown in Fig. 5. Since we rely on the dispersion of the D-lines for phase matching and resonance enhancement of $\chi^{(Q)}$, we cannot tune very far from the D-lines, and the density must ~~therefore~~ be limited to 10^{17} cm^{-3} or less. In addition, Na_2 absorp-

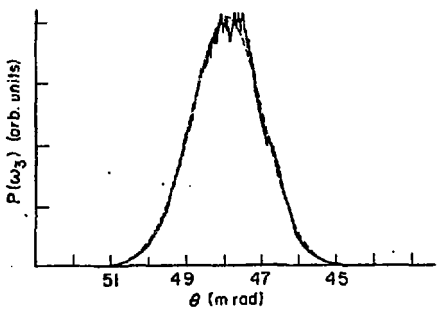

Figure 4: Phase-matching curve $\mathcal{P}(\omega_3)$ versus θ. $\mathcal{P}_1 = 2$W; $\mathcal{P}_2 = 25$W; $\Delta\omega_1 \equiv \omega_{3P_{\frac{1}{2}}} - \omega_1 = 25.6$ cm^{-1}; $\omega_1 + \omega_2 = \omega_{4d}$; $N = 1.6 \times 10^{16}$ cm^{-3}. The dashed curve is a theoretical curve calculated from Eq. (4).

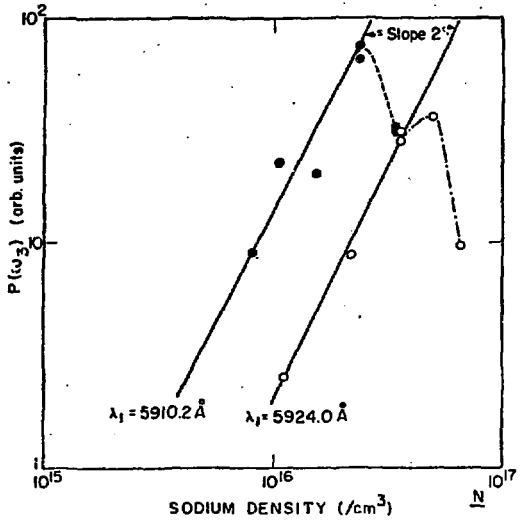

Figure 5: Phase-matched sum-frequency output $\mathcal{P}(\omega_3)$ as a function of sodium density N at $\Delta\omega_1 = 40.8$ cm^{-1} and 80.4 cm^{-1}. The other parameters fixed in the experiment are $\mathcal{P}_1 = 2W$, $\mathcal{P}_2 = 20W$, and $\omega_1 + \omega_2 = \omega_{4d}$.

tion increases strongly at densities above 10^{17}.

A second limiting factor is two-photon saturation. Since the output power is proportional to the square of the population difference between the 3s and 4d states, we have

$$\mathcal{P}(\omega_3) \propto [1/W_{tp}T]^2 , \qquad (5)$$

where W_{tp} is the two-photon excitation rate from 3s to 4d and T is an effective upper-state relaxation time. For Gaussian beams the spatial variation of the intensities must be considered, and in this case

$$\mathcal{P}(\omega_3) \propto \frac{I_1 I_2}{|\Delta\omega_2|^2} \int_{-\infty}^{\infty} \frac{dy}{e^{y^2} + \frac{wI_1I_2}{|\Delta\omega_2|^2}}, \qquad (6)$$

where w is a constant related to the two-photon transition probability and $\Delta\omega_2 = \omega_{4d} - \omega_1 - \omega_2 - i\gamma$. Eq. (6) predicts both saturation of the output with increasing $I_1 \cdot I_2$, and broadening of the two-photon resonance curve. In Fig. 6 we compare these predicted variations with the experimentally observed saturation and broadening. The constant, w, was chosen to give the best fit to the saturation data. The fit value, $w = 1.55 \times 10^{-3}$ is in satisfactory agreement with the theoretical value $w = 1.2 \times 10^{-3}$. Saturation of the signal on two-photon resonance becomes significant for $I_1 I_2 \approx 10^{11} w^2/cm^4$, for an intermediate state detuning of 41.2 cm^{-1}.

Finally, at high intensities, third order nonlinearities and population redistribution can cause changes in the index of refraction of the vapor which defocus the pump beams and, more importantly, destroy the phase matching of the output radiation. By measuring the defocusing of the beam nearest the D lines, we deduce that induced changes of the refractive index for that beam may be on the order of 10^{-5}. Both theoretical estimates and experiment show that index changes of that magnitude are sufficient to reduce the output substantially below the value expected if no induced index changes were present. A refractive index change of this magnitude is produced in Na by an intensity as low as 1 MW/cm^2 at 40 cm^{-1} detuning from the D lines and a pressure of 2 torr, by saturation of the dispersion. It can also be produced by fractional ionization (due to resonant multiphoton ionization) of only one percent. Such index changes are the strongest factors limiting conversion efficiency in our sum-frequency generation experiments.[3]

Besides frequency mixing, quadrupole sum-frequency generation also allows us to use a novel and accurate technique to measure quadrupole transition moments of atoms and molecules.[4] The technique uses the interference of quadrupole sum-frequency generation and DC field-induced third order sum-frequency generation to allow direct comparison of the quadrupole moment with products of dipole moments. Since the dependence of the two processes on the beam geometry and intensities, phase matching, and atomic density are all common, only the matrix elements themselves are compared. Thus, we expect the technique to be capable of high accuracy.

To describe the interference theoretically, the total effective polarization radiating in the direction $\underline{k}_3$ is written:

$$\underline{P} = [-i\underline{k}_3 \cdot \underline{\chi}^{(Q)} + \underline{\chi}^{(3)} \cdot \underline{E}_0] : \underline{E}_1\underline{E}_2, \qquad (7)$$

where E_0 is the DC field. This polarization is proportional to:

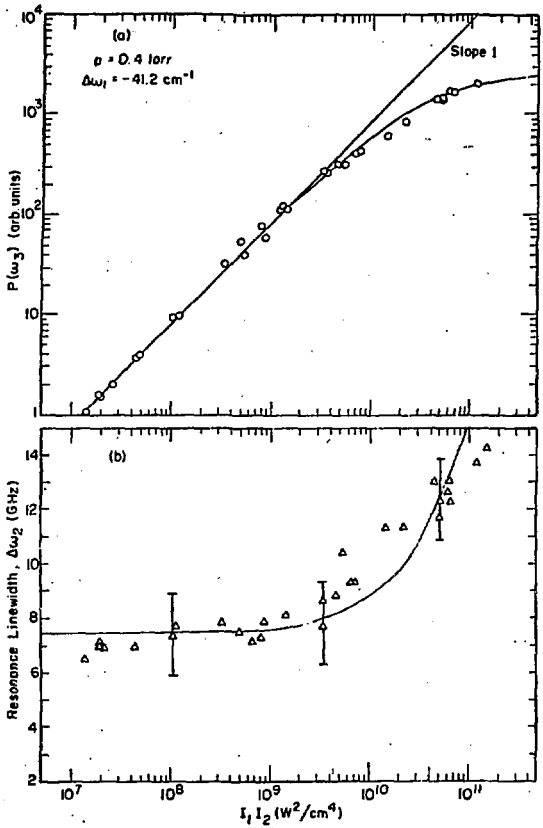

Fig. 6: (a) Sum-frequency power $P(\omega_3)$ and (b) resonance linewidth $\Delta\omega_2$ as functions of the product of the input intensities $I_1 I_2$. The solid curves are both derived from Eq. (6) for the effects of two-photon saturation with $w = 1.55\times10^{-9}$.

$$\underline{P} \propto [-i\underline{k}_3 \cdot \underline{M}_Q + \underline{M}_D \cdot \underline{E}_0] \ , \tag{8}$$

where:

$$\underline{M}_Q = \langle a|\underline{r}\ \underline{r}/2|b\rangle$$

$$\underline{M}_D = e\sum_c \left[\frac{-\langle a|\underline{r}|c\rangle\langle c|\underline{r}|b\rangle}{\hbar(\omega_3 - \omega_c)} + \frac{\langle c|\underline{r}|b\rangle\langle a|\underline{r}|c\rangle}{\hbar\omega_c}\right] .$$

When E_0 is adjusted and both light fields are linearly polarized, the output is *circularly* polarized when:

$$E_0 = \pm k_3 M_{Qzz} \tan\theta_2 / M_{Dzz} \ , \tag{9}$$

where θ_2 is the angle between $\underline{k}_2$ and $\underline{k}_3$. When the ω_2 input beam is circularly polarized, the component of the output parallel to $\underline{k}_2 \times \underline{k}_2$ has a minimum at a field

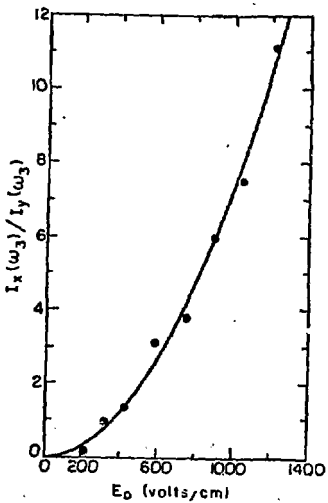

Figure 7: $I_x(\omega_3)/I_y(\omega_3)$ as a function of the applied DC field E_0 for linear polarized input beams. $I_x(\omega_3)$ and $I_y(\omega_3)$ are phase-matched sum-frequency signals polarized along $\hat{x}$ and $\hat{y}$, respectively. The solid curve is a theoretical curve obtained from Eq.(7) to fit the data points.

$$E_0 = 3/4(k_3 M_{Qzz} \sin\theta_z / M_{Dzz}). \quad (10)$$

Either condition allows us to determine (M_Q/M_D), including sign, if we know the electric field strength. To demonstrate this technique, we have measured the 3s-4d quadrupole transition moment of the sodium atom. E_0 was applied with a pair of flat plate electrodes, heated to prevent Na condensation. The results for linearly polarized input light are shown in Fig. 7, while those for one input beam circularly polarized are shown in Fig. 8. Using tabulated values for the dipole matrix elements, we derive the values $\langle 3s|zz/2|4d\rangle = +2.24a_0^2$ and $\langle 3s|zz/2|4d\rangle = +2.27a_0^2$, respectively, from the two measurements. Laser fluctuations limited our accuracy in this experiment to about ±20%.

We have so far considered the sum-frequency generation process in which mixing of two pump beams at ω_1 and ω_2 induces a quadrupole polarization at $\omega_3 = \omega_1 + \omega_2$. Another interesting possibility involves the creation of an electric *dipole* polarization by mixing of two *pump fields*, one of which is coupled to a quadrupole transition. Because the transition is so weak, a laser can be tuned directly to

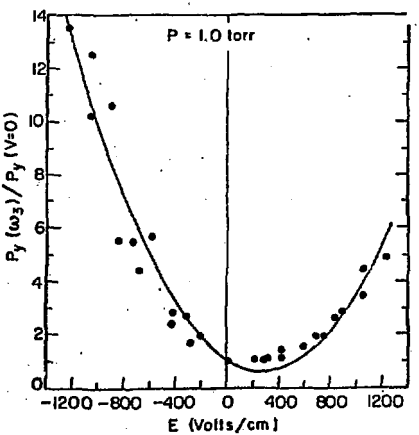

Figure 8: $I_y(\omega_3)/I_y(\omega_3, E_0 = 0)$ as a function of the applied DC field E_0 for $\underline{E}(\omega_1)$ linearly polarized along y and $\underline{E}(\omega_2)$ left circularly polarized.

the quadrupole transition to achieve maximum resonant enhancement. Such a process can be described by the *difference* frequency polarization

$$\underline{P}(\omega_1 - \omega_2) = i\chi^{(Q_1)}[\underline{E}_1(\underline{k}_1 \cdot \underline{E}_2^*) + \underline{k}_1(\underline{E}_1 \cdot \underline{E}_2^*)] \ , \qquad (11)$$

where

$$\chi^{(Q_1)} = \frac{Ne^3}{\hbar^2} \sum_{rst} \frac{\langle r|z|s\rangle\langle s|y|t\rangle\langle t|zy/2|r\rangle}{(\omega_{sr} - \omega_2)(\omega_{tr} - \omega_1)} \ .$$

As an example, if we tune two lasers near the 6s-6d quadrupole and 6s-7p dipole transitions of cesium vapor, we should obtain infrared difference frequency generation in the range 14-15μ near the 7p-6d dipole allowed transition of the atoms. For $N = 10^{17}cm^{-3}$, $\omega_{7p_{3/2}} - \omega_2 = 2cm^{-1}$ and $\omega_{6d_{5/2}} - \omega_1 = .25\ cm^{-1}$ we find $\chi^{(Q_1)} = 2.1 \times 10^{-12}$ esu and $\mathcal{P}(\omega_3) = \mathcal{P}(\omega_1)\mathcal{P}(\omega_2)/15$MW. μW.

The inclusion of higher multipole terms in the interaction of light with matter allows second order nonlinear processes to be observed in isotropic media. These processes may be useful both for generating new wavelengths of radiation, and for measuring atomic or molecular quadrupole transition moments, which are difficult to measure using other techniques. We may thus observe and exploit weak transitions, which until recently, were routinely neglected.

insert here

References

1. D. S. Bethune, R. W. Smith and Y. R. Shen, Phys. Rev. Letts. *37*, 431 (1976).
2. P. S. Pershan, Phys. Rev. *130*, 919 (1963); E. Adler, Phys. Rev. *134*, A728 (1964).
3. Further details on these measurements to be published in Phys. Rev. A.
4. D.S. Bethune, R.W. Smith and Y.R. Shen, Phys. Rev. Letts. *38*, 647 (1977).

* This work was done with support from the U.S. Energy Research and Development Administration.